

Annealing Effects of Iron Nitride Thin Film Grown by Plasma-Assisted Evaporation Technique

Nobuyasu ADACHI, Masaki ENDO, Noboru MENJO and Takashi OKUDA

Department of Materials Science and Engineering, Nagoya Institute of Technology, Gokiso-cho, Showa-ku, Nagoya-shi 466-8555

プラズマ真空蒸着法により作製した窒化鉄膜の熱処理効果

安達信泰・遠藤正樹・校条 昇・奥田高士

名古屋工業大学材料工学科, 466-8555 名古屋市昭和区御器所町

Fe-N films were synthesized by a plasma-assisted deposition technique and annealing effects were investigated. X-ray diffraction (XRD) showed that the as-deposited films consist of the Fe_xN ($2 \leq x \leq 3$) mixed phases. After annealing the as-deposited film at 500°C , the saturation magnetization increased to 2.5 Wb/m^2 which is larger than that of pure Fe ($4 \pi M_s = 2.1 \text{ Wb/m}^2$). The XRD patterns of the film annealed at 500°C indicated the existence of Fe_4N and Fe or Fe_{16}N_2 phases where the diffraction patterns of Fe and Fe_{16}N_2 could not be distinguished from each other, however, the diffraction patterns obtained by transmission electron microscopy (TEM) confirm the formation of Fe_{16}N_2 phase in the film.

[Received August 7, 2002; Accepted March 24, 2003]

Key-words : Fe_{16}N_2 , Iron nitride, Annealing, High saturation magnetization

1. Introduction

Kim and Takahashi found that Fe-N films deposited by an evaporation method in reduced N_2 gas atmosphere exhibited a high saturation magnetization of $4 \pi M_s = 2.6 \text{ Wb/m}^2$, which is much higher than that of pure α -iron ($4 \pi M_s = 2.1 \text{ Wb/m}^2$).¹⁾ Since then, Fe_{16}N_2 has attracted much attention as a phase with a large magnetic moment. A number of researchers have attempted to form Fe_{16}N_2 using different techniques; the reproduction of the film with the giant magnetic moment had not been obtained. In 1988, by using the molecular beam epitaxy (MBE) technique, Komuro et al. successfully synthesized single-crystal Fe_{16}N_2 films with giant magnetic moment of 2.9 Wb/m^2 at room temperature.²⁾ Therefore, it was confirmed that Fe_{16}N_2 has higher saturation magnetization than that of iron. Also, Nakajima et al. formed Fe_{16}N_2 in epitaxial iron films by nitrogen implantation.³⁾ In contrast to these reports, Takahashi et al. pointed out that there is no marked increase of $4 \pi M_s$ in Fe_{16}N_2 and the value of $4 \pi M_s$ at room temperature is 2.23 Wb/m^2 .⁴⁾ According to the theoretical calculations, Sakuma estimated the magnetic moment of the Fe atom in Fe_{16}N_2 to be $2.39 \mu_B$ (μ_B is Bohr magneton), which corresponds to only 2.17 Wb/m^2 , from the local spin density (LSD) functional theory.⁵⁾ On the other hand, Lai et al. estimated it to be $2.85 \mu_B$, which corresponds to 2.58 Wb/m^2 , from the local density approximation considering Coulomb interaction.⁶⁾ The experimental results for the films prepared by different growth techniques and growth conditions have been compared and they do not agree with each other. Theoretical calculations have been performed using different models and the estimated results also indicated different values. The large $4 \pi M_s$ and the true magnetic moment of the Fe atom in Fe_{16}N_2 are still subjects of current controversy.^{2),7),8)}

For practical applications, however, it is important to improve crystal growth techniques of Fe_{16}N_2 because this material is expected to be a soft magnetic material with magnetic moment larger than Fe. For practical use, MBE, which is the conventional growth technique for synthesizing Fe_{16}N_2 thin film, has the disadvantage of a very low deposition rate ($1\text{--}20 \text{ nm/h}$).⁹⁾

We report the possibility of synthesizing Fe_{16}N_2 phase by

annealing films with Fe_xN ($2 \leq x \leq 3$) mixed phases prepared by a plasma-assisted evaporation technique. One of the films showed a large value of $4 \pi M_s = 2.5 \text{ Wb/m}^2$ which was annealed at 500°C . The growth technique is simple and the deposition rate is 200 nm/h which is much higher than that of the MBE technique. In the preparation process, a film with Fe_xN ($2 \leq x \leq 3$) mixed phases was synthesized by plasma-assisted evaporation, and then the as-deposited film was annealed to denitrify the nitrogen rich film. We expect the formation of Fe_{16}N_2 under an optimal annealing condition. In this report, the deposition and annealing processes are described in detail.

2. Experimental

Fe-N films were prepared by plasma-assisted evaporation onto Mo substrates with 0.1 mm thickness and $5 \times 5 \text{ mm}^2$ size. Evaporation of Fe(99.5%) was carried out using a spiral-shaped tungsten filament covered with Al_2O_3 . The nitrogen gas was introduced into the vacuum chamber evacuated under $1.3 \times 10^{-4} \text{ Pa}$. N_2 plasma was generated by discharging nitrogen gas near the substrate using induction coil power supply. During deposition, the pressure of N_2 gas was held at 20 Pa and the substrate temperature was kept at 200°C . After deposition, the substrate was cooled to room temperature in the plasma gas. The deposition rate was between 2 and 4 nm/min . The thickness of the films used for characterization is usually from 100 to 300 nm , which was measured with a needle contact feeler gauge and was confirmed by the cross section observed by using a transmission electron microscopy (TEM).

Annealing treatments were carried out in an infrared furnace with a base pressure of $2.7 \times 10^{-4} \text{ Pa}$. The films were heated for 1 hour at various annealing temperatures (T_{anneal}) ranging from 200 to 500°C . The heating and cooling rate was about 10°C/min .

The crystal phases of the films were analyzed by X-ray diffraction (XRD) with $\text{Cu K}\alpha$ radiation and by using a TEM. The specimen for the plain view and the cross section observation was prepared by mechanical polishing and the ion milling technique. After fabricating the film on the substrate with $5 \times 5 \times 0.5 \text{ mm}^3$ size, the specimen was mounted on a Mo ring with 2 mm diameter. The diffraction pattern

was obtained from the plain view observation and the thickness of the film was confirmed by the cross section observation. Magnetization was measured by using a vibrating sample magnetometer (VSM) in the temperature range between room temperature and 500°C. The base pressure was 6.7×10^{-3} Pa and the working pressure was approximately 1×10^{-2} Pa.

3. Results and discussion

The XRD θ - 2θ patterns of the as-deposited and the annealed films are shown in Fig. 1. No diffraction peak from Fe phase was observed and the diffraction peak at approximately around at 42.8° in Fig. 1(a) was assigned to be the diffraction peak from the 211 Fe_2N phase. This peak position is known to shift continuously to the 101 Fe_3N peak position with decreasing nitrogen content. At the shoulder of the Mo diffraction peak, the 002 Fe_2N diffraction peak seems to be hidden at approximately 41° . The shoulder of 211 Fe_2N is considered to be due to the diffraction from the Fe_xN ($2 < x < 3$) phase. The films deposited in approximately 20 Pa atmosphere usually consist of Fe_xN ($2 \leq x \leq 3$) phase. As T_{anneal} increased, the diffraction peak at approximately 43.8° gradually shifted to approximately 44.8° (see Fig. 1(c)). The diffraction peak at 44.8° corresponds to either the Fe_{16}N_2 220 peak position or the Fe 110 peak position, however we were unable to distinguish them from each other. In addition, other diffraction peaks appear at approximately 41.3° (see Fig. 1(b)), 48.2° and 70.4° (see Fig. 1(c)) which were assigned to be Fe_4N 111, 200, and 220 diffraction peaks, respectively. The peak at 82.3° corresponds to the Fe_{16}N_2 422 peak position and the Fe the 211 peak position. According to a calculation and the powder patterns of α - Fe_{16}N_2 , the 220 diffraction peak has the highest intensity.^{10),11)} In Fig. 1, the 220 peak is not observed. The reason for the different results is not understood yet. In the data obtained by Jack who first analyzed the α - Fe_{16}N_2 phase,¹¹⁾ the 220 peak was also not observed. One of the possible reasons for our result is that the diffraction peaks that appeared at 44.8° and 82.3° are mainly due to crystallized Fe phase and the diffraction due to the Fe_{16}N_2 phase is weak. There is also the possibility that the intermediate phase of ordered α '- Fe_{16}N_2 and α '-disordered phase is formed which reduces the peak intensity. These discussions are described further in the following TEM results.

Figure 2 shows T_{anneal} dependence of saturation magnetization $4\pi M_s$ of the films. The $4\pi M_s$ of the as-deposited film was approximately 1.0 Wb/m². The $4\pi M_s$ of Fe_3N is below 1.4 Wb/m². From the value of $4\pi M_s$, the temperature dependence of the magnetization of the as-deposited film (shown in Fig. 4) and the XRD patterns, the main phase in the as-deposited film is thought to be Fe_3N . The $4\pi M_s$ decreased after the film was annealed at 300°C, the reason for this is not apparent at the present stage. The $4\pi M_s$ of the film increased with increasing T_{anneal} above 300°C. It suggests that nitrogen in Fe-N films was dissociated by annealing. The film annealed at 500°C showed a maximum of $4\pi M_s = 2.5 \pm 0.2$ Wb/m² which was higher than that of pure iron ($4\pi M_s = 2.1$ Wb/m²). One of the possible reasons for the high saturation magnetization is the formation of Fe_{16}N_2 phase, however, the dynamics of the formation of the Fe_{16}N_2 phase by this deposition and annealing technique is not clear at the present stage.

The electron diffraction pattern of this film obtained by TEM observation is shown in Fig. 3. The ring pattern indicates polycrystalline film. The broad ring may be due to a wide distribution of crystal size or fine grain structure in the film. The diffraction pattern indicates the presence of Fe_4N , Fe_{16}N_2 and Fe phases in the film. Around the ring positions of Fe_{16}N_2 220 and 202, a broad ring was observed. In this

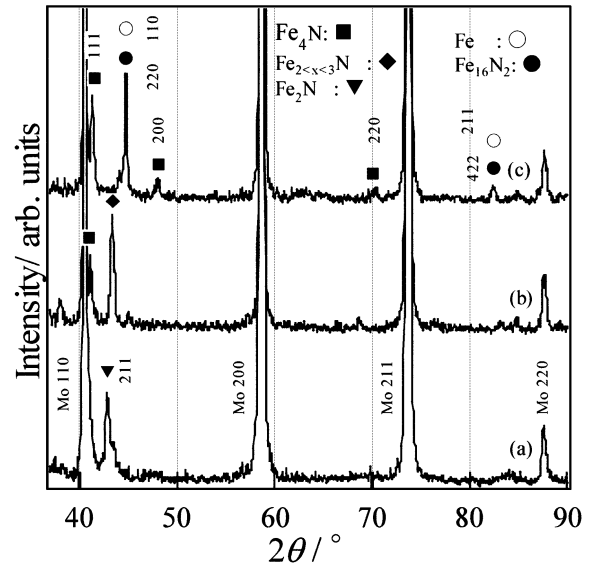


Fig. 1. XRD patterns of Fe-N films. (a) As-deposited, (b) annealed at 400°C and (c) annealed at 500°C.

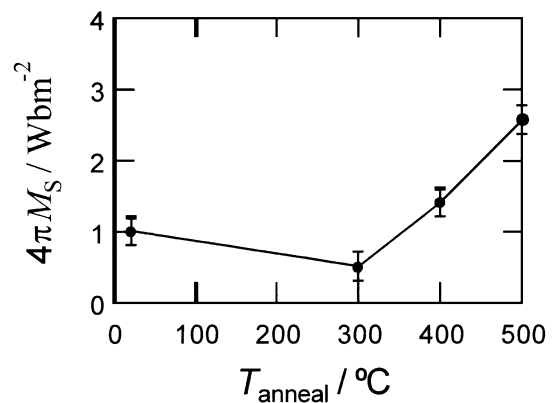


Fig. 2. T_{anneal} dependence of $4\pi M_s$.

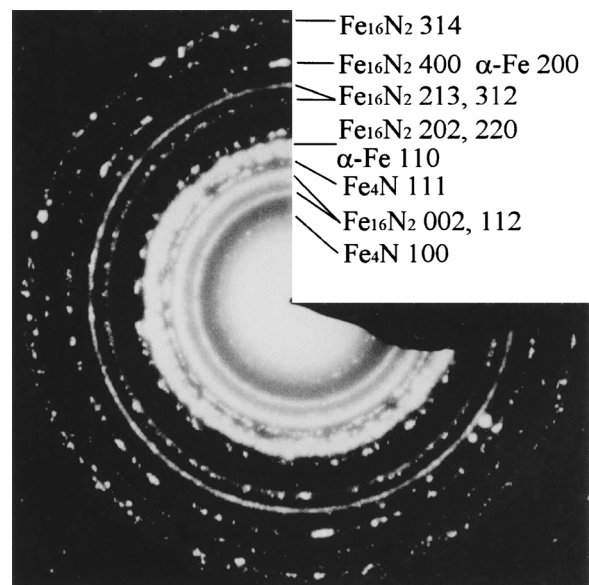


Fig. 3. Electron diffraction pattern of Fe-N film with high $4\pi M_s = 2.5$ Wb/m².

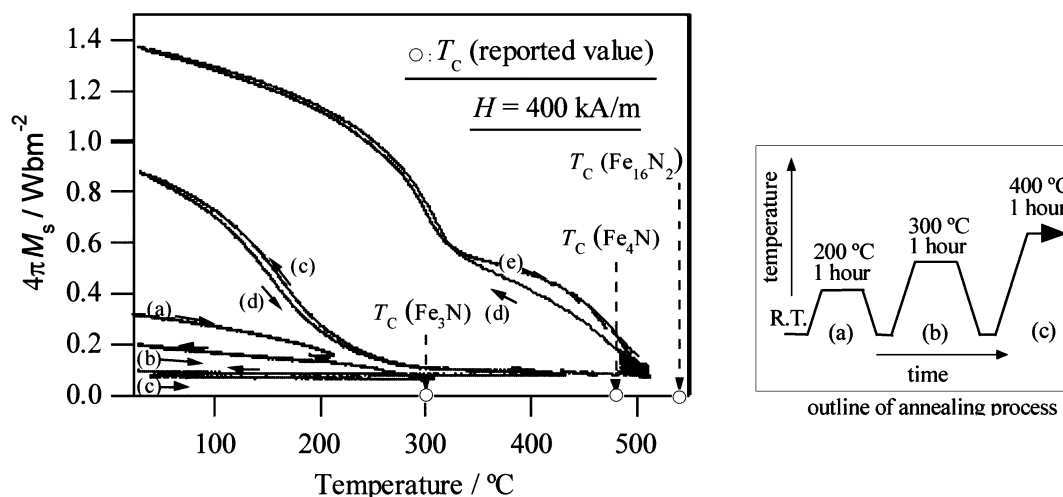


Fig. 4. Temperature dependence of the magnetization of the Fe-N film in the magnetic field of 400 A/m. The schematic of the heating process is also shown. The sample was fixed in a fused-silica glass holder in vacuum atmosphere and the temperature was increased to (a) 200°C, (b) 300°C, (c) 400°C and (d) 500°C after cooling to room temperature at each step.

figure, the 002, 112 and 314 diffraction rings due to Fe_{16}N_2 were recognized, which were not observed in the XRD pattern in Fig. 1. These diffractions come from only the Fe_{16}N_2 phase. Judging from the TEM diffraction pattern, the existence of Fe_{16}N_2 phase probably results in a large $4\pi M_s$ value of the film. The inconsistency between XRD and TEM results is not clear at the present stage. In our data, the absolute intensities of polycrystalline XRD peaks are often small for the Fe-N film with approximately 100 nm thickness. The TEM observation is a advantageous for investigating the local area in order to confirm the existent phases.

Figure 4 shows the temperature dependence of magnetization of the Fe-N film in a magnetic field of 400 kA/m. The heat treatment was performed as follows. The temperature of the film was increased from room temperature to T_{anneal} and was kept at T_{anneal} for 1 h; then it was decreased to room temperature. T_{anneal} was set at 200, 300, 400 and 500°C and a sequence of the procedure was performed continuously. The $4\pi M_s$ of the as-deposited film was 0.3 Wb/m² at room temperature. The low saturation magnetization suggests that the film consisted of Fe_2N paramagnetic phase. With increasing temperature to 200°C, the magnetization of the film gradually decreased (see Fig. 4(a)). The magnetization curve between the heating and cooling process was irreversible. After cooling from $T_{\text{anneal}} = 300^\circ\text{C}$ (see Fig. 4(b)), the $4\pi M_s$ became 0.1 Wb/m² at room temperature. After cooling from $T_{\text{anneal}} = 400^\circ\text{C}$ (see Fig. 4(c)), magnetization rapidly increased at approximately 300°C and the $4\pi M_s$ at room temperature became 0.9 Wb/m². Taking it into consideration the fact that the Curie temperature (T_c) of the Fe_3N is approximately 300°C, the annealing process (c) formed Fe_3N . The magnetization curve in the cooling process from 500°C shows two steps which suggest two phases with different T_c in the film (see Fig. 4(d)). With increasing to 500°C again, the magnetization curve also showed two steps reversibly. These values of T_c were estimated to be approximately 350 and 520°C. The former was larger than that of T_c of Fe_3N ($T_c \approx 300^\circ\text{C}$) and smaller than the T_c of Fe_4N ($T_c = 488^\circ\text{C}$). The latter seemed to be over the T_c of Fe_4N and slightly smaller than the T_c of Fe_{16}N_2 ($T_c = 540^\circ\text{C}$). Taking the diffraction pattern in Fig. 3 into account, Fe_4N and Fe_{16}N_2 phases were expected to form in the film heated at 500°C and the two steps of the M - T curve represent the contribution of mixed phases.

However, the estimated T_c did not completely agree with the T_c of Fe_4N and Fe_{16}N_2 and the reason for the disagreement is not clear yet. The M - T measurements were performed above 10^{-3} Pa and some contamination in the film should be allowed. The maximum $4\pi M_s$ of less than 2.5 Wb/m² may be one of the reasons for the contamination during heating at low vacuum pressure.

4. Conclusion

The Fe-N film was synthesized by plasma-assisted deposition. It was confirmed that the Fe_{16}N_2 phase was formed by annealing the Fe_xN ($x \leq 4$) film at 500°C. The film consisted of mixed Fe_xN phases, however, the maximum $4\pi M_s$ reached 2.5 Wb/m², which is much larger than that of α -Fe. This indicates that annealing Fe_xN ($x \leq 4$) is an effective technique for forming Fe_{16}N_2 phase.

Acknowledgements The authors would like to thank Professor Kazuhiro Hono of the National Institute of Materials Science for helping with TEM observation.

References

- Kim, T. K. and Takahashi, M., *Appl. Phys. Lett.*, Vol. 20, pp. 492-494 (1972).
- Komuro, Y., Kozono, Y., Hanazono, M. and Sugita, Y., *J. Appl. Phys.*, Vol. 67, pp. 5126-5130 (1990).
- Nakajima, K., Okamoto, S. and Okada, T., *J. Appl. Phys.*, Vol. 65, pp. 435743-435761 (1989).
- Takahashi, M., Shoji, H., Takahashi, H., Wakiyama, T., Kinoshita, M. and Ohta, M., *IEEE Trans. Magn.*, Vol. 29, pp. 3040-3045 (1993).
- Sakuma, A., *J. Magn. Magn. Mater.*, Vol. 102, pp. 127-134 (1991).
- Lai, W. Y., Zheng, Q. Q. and Hu, W. Y., *J. Phys. Condens. Matter.*, Vol. 6, pp. L259-L264 (1994).
- Takahashi, H., Komuro, M., Hiratani, M. and Igarashi, M., *J. Appl. Phys.*, Vol. 84, pp. 1493-1498 (1998).
- Takahashi, M., Shoji, H., Takahashi, H., Nashi, H., Wakiyama, T., Doi, M. and Matsui, M., *J. Appl. Phys.*, Vol. 76, pp. 6642-6647 (1994).
- Sugita, Y., Mitsuoka, K., Komuro, M., Hoshiya, H., Kozono, Y. and Hanazono, M., *J. Appl. Phys.*, Vol. 70, pp. 5977-5982 (1991).
- Nagatomi, A., Yoshikawa, S., Hinomura, T., Nasu, S. and Kanamaru, F., *J. Jap. Soc. Powder & Powder Metall.*, Vol. 46, pp. 151-155 (1999).
- Jack, K. H., *Proc. Roy. Soc. London, Ser.*, Vol. A 208, pp. 215-224 (1951).